

# Electronic Supporting Information for

## Cancer Phototherapy by CO Releasing Terpyridine-Based Re(I) Tricarbonyl Complexes via ROS Generation and NADH Oxidation

*Rajesh Kushwaha,<sup>a</sup> Aarti Upadhyay,<sup>b</sup> Sukanta Saha,<sup>c</sup> Ashish Kumar Yadav,<sup>a</sup> Arpan Bera,<sup>\*b</sup>  
Arnab Dutta,<sup>c</sup> Samya Banerjee,<sup>\*a</sup>*

- a R. Kushwaha, A. K. Yadav, and Dr. S. Banerjee  
Department of Chemistry  
Indian Institute of Technology (BHU), Varanasi  
Uttar Pradesh India 221005  
E-mail: samya.chy@itbhu.ac.in
- b A. Upadhyay and A. Bera  
Department of Inorganic and Physical Chemistry  
Indian Institute of Science, Bangalore  
E-mail: arpanbera@iisc.ac.in
- c S. Saha and A. Dutta  
Department of Chemistry  
Indian Institute of Technology Bombay, Mumbai  
Maharashtra 400076, India

## Table of Contents

|  |     |
|--|-----|
| Materials  | S4  |
| Instruments  | S4  |
| Synthesis  | S4  |
| Methods  | S6  |
| <b>Tables:</b>   |     |
| <b>Table S1.</b> Crystal data parameters and refinement details of <b>Retp1</b> and <b>Retp2</b> .               | S10 |
| <b>Table S2:</b> Selected bond lengths (Å) and bond angles (°).  | S11 |
| <b>Table S3.</b> Energy (eV) of the lowest vertical 10 singlet–singlet transitions of <b>Retp1-Retp3</b> .       | S12 |
| <b>Table S4.</b> Energy (eV) of the lowest vertical 10 singlet–Triplet transitions of <b>Retp1-Retp3</b> .       | S12 |
| <b>Figures:</b>  |     |
| <b>Figure S1.</b> <sup>1</sup> H NMR spectra of <b>Retp1</b> .   | S12 |
| <b>Figure S2.</b> <sup>1</sup> H NMR spectra of <b>Retp2</b> .   | S13 |
| <b>Figure S3.</b> <sup>1</sup> H NMR spectra of <b>Retp3</b> .   | S13 |
| <b>Figure S4.</b> <sup>13</sup> C NMR spectra of <b>Retp1</b> .  | S14 |
| <b>Figure S5.</b> <sup>13</sup> C NMR spectra of <b>Retp2</b> .  | S14 |
| <b>Figure S6.</b> <sup>13</sup> C NMR spectra of <b>Retp3</b> .  | S15 |
| <b>Figure S7.</b> FT-IR spectra of <b>Retp1</b> .  | S15 |
| <b>Figure S8.</b> FT-IR spectra of <b>Retp2</b> .  | S16 |
| <b>Figure S9.</b> FT-IR spectra of <b>Retp3</b> .  | S16 |
| <b>Figure S10.</b> HRMS spectra of <b>Retp1</b> .  | S17 |
| <b>Figure S11.</b> HRMS spectra of <b>Retp2</b> .  | S17 |
| <b>Figure S12.</b> HRMS spectra of <b>Retp3</b> .  | S18 |
| <b>Figure S13:</b> Representative figure for Unit cell packing of <b>Retp1</b> .                                 | S18 |
| <b>Figure S14:</b> Representative figure for Unit cell packing of <b>Retp2</b> .                                 | S19 |
| <b>Figure S15.</b> Selected frontier molecular orbitals (FMOs) for the <b>Retp1</b> .                            | S19 |
| <b>Figure S16.</b> Selected frontier molecular orbitals (FMOs) for the <b>Retp2</b> .                            | S20 |
| <b>Figure S17.</b> Selected frontier molecular orbitals (FMOs) for the <b>Retp3</b> .                            | S20 |
| <b>Figure S18:</b> S1 optimized geometries of <b>Retp1-Retp3</b> .   | S21 |
| <b>Figure S19:</b> T1 optimized geometries of <b>Retp1-Retp3</b> .   | S21 |
| <b>Figure S20.</b> Calculated frontier orbital energies of ground states of <b>Retp1-Retp3</b> .                 | S21 |
| <b>Figure S21.</b> Vertical energy levels of <b>Retp1-Retp3</b> for singlet (S1) and triplet (T1) excited state. | S22 |

|  |     |
|--|-----|
| <b>Figure S22:</b> $^1\text{O}_2$ generation induced by <b>Retp1-Retp3</b> (10 $\mu\text{M}$ ) under the dark condition.                       | S22 |
| <b>Figure S23:</b> $^1\text{O}_2$ generation induced by <b>[Ru(bpy)<sub>3</sub>]Cl<sub>2</sub></b> (10 $\mu\text{M}$ ) upon light irradiation. | S22 |
| <b>Figure S24:</b> $\text{OH}^\bullet$ generation induced by <b>Retp1-Retp3</b> under dark conditions.   | S23 |
| <b>Figure S25:</b> NADH oxidation by <b>Retp1</b> and <b>Retp2</b> in the visible light condition.   | S23 |
| <b>Figure S26:</b> Stability plot for <b>Retp3</b> under the dark condition.   | S23 |
| <b>Figure S27:</b> Stability plot for <b>Retp3</b> in the presence of GSH.   | S24 |
| <b>Figure S27:</b> Cell viability plots for complexes <b>Retp1-Retp3</b> in A549 cells.  | S24 |
| <b>Figure S28:</b> Cell viability plots for complexes <b>Retp1-Retp3</b> in HeLa cells.  | S24 |
| <b>Figure S29:</b> Cell viability plots for complexes <b>Retp1-Retp3</b> in Beas-2B cells.   | S25 |
| <b>Figure S30:</b> Cell viability plots for cisplatin in Beas-2B cells.  | S25 |
| References   | S25 |

## Materials:

Rhenium pentacarbonyl chloride,  $\text{Re}(\text{CO})_5\text{Cl}$ , and acetyl pyridine were purchased from Merck. Benzaldehyde, anthracene-carboxaldehyde, and pyrene-carboxaldehyde were obtained from TCI Chemicals. KOH, aq. Ammonia and Toluene were obtained from SRL Chem. Diethyl-ether, Hexane, DCM, and ethanol were purchased from Merck Life Science Private Limited. 1,3-Diphenylisobenzofuran, 9,10-Diphenylanthracene (DPA), 2',7'-Dichlorodihydrofluorescein diacetate (DCFHDA) and  $\beta$ -Nicotinamide adenine dinucleotide, reduced disodium salt ( $\beta$ -NADH) were purchased from Sigma Aldrich. Quantofix peroxide test sticks were purchased from Sigma Aldrich. Dulbecco's Phosphate Buffered Saline was purchased from Sigma Aldrich. A549, HeLa, and Beas-2B cell lines were procured from NCCS Pune India. Dulbecco's Modified Eagle Medium (DMEM) and 12 well cell culture plates were purchased from Genetix Pvt. Ltd. T-25 flask and 96 well plates were obtained from Eppendorf. 12 well cell culture plates were obtained from Genetix Biotech Asia Pvt. Ltd. FBS (Fetal Bovine Serum), Trypsin-EDTA, and Penicillin-streptomycin were procured from Gibco. JC-1 and Annexin V-FITC/PI Apoptosis Detection Kit were purchased from Genetix Biotech Asia Pvt.

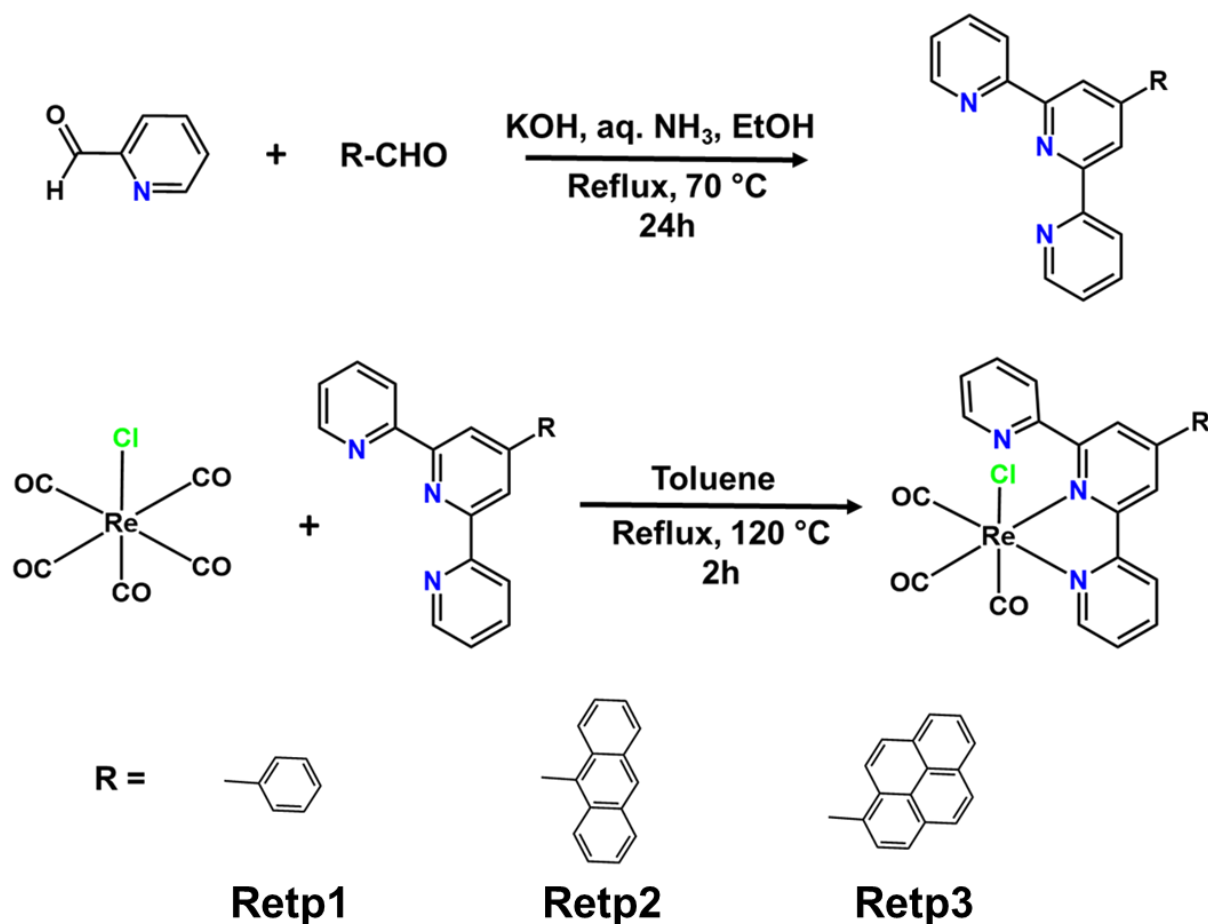
## Instrumentation

Agilent Cary 60 UV-Vis spectrophotometer was used for recording the UV-vis spectral data. MaXis impact 282001.00081 was used for the HR-MS. Fluorescence measurements were performed on a Techcomp FL970 fluorescence spectrophotometer. Luzchem-ICH2 photoreactor (400-700 nm) was used for light-activated studies. In the 3-(4,5-dimethylthiazol-2-yl)-2,5-diphenyltetrazolium bromide (MTT) assay, the absorbance value of formazan was recorded using a TECAN microplate reader, and the graph was plotted using GraphPad Prism 6 software. Flow cytometric experiments were performed using Becton Dickinson fluorescent-activated cell sorting (BD-FACS) Verse instrument (BD Biosciences). FACS analysis data acquisition and analysis were done using Windows 7 operating system and BD-FACS suite software. Confocal laser scanning microscopy (CLSM) was done using a Zeiss LSM 880 with Airyscan microscope containing an oil immersion lens. Confocal microscopic images of the JC-1 assay were taken at a magnification of 10X, and co-localization images were taken at the magnification of 63x.

## Synthesis:

### General synthetic procedure:

4'-phenyl-2,2':6',2''-terpyridine (ph-tpy), 4'-anthracenyl-2,2':6',2''-terpyridine (an-tpy), and 4'-pyrenyl-2,2':6',2''-terpyridine (py-tpy) were synthesized according to the method described in the literature.<sup>1</sup> 1.0 equivalent of terpyridine-based ligands (4'-phenyl-2,2':6',2''-terpyridine (in **Retp1**), 4'-anthracenyl-2,2':6',2''-terpyridine (in **Retp2**), and 4'-pyrenyl-2,2':6',2''-terpyridine (in **Retp3**)) and 1.0 equivalent of  $\text{Re}(\text{CO})_5\text{Cl}$  were dissolved in 10-15 mL of Toluene.<sup>2</sup> The reaction mixture was refluxed for 2 h under inert conditions. After 1-1.5 h, precipitation formation was started. The precipitated complexes were filtered, washed with hexane and  $\text{Et}_2\text{O}$ , and dried under vacuum conditions over  $\text{P}_4\text{O}_{10}$ . The complexes were recrystallized from the DCM-ethanol mixture.



**Reaction Scheme S1:** Synthetic route for the synthesis of ligands and **Retp1-Retp3**.

**Retp1:** Yellow solid. 90% yield. C<sub>24</sub>H<sub>15</sub>ClN<sub>3</sub>O<sub>3</sub>Re (MW = 615.06 g/mol) calcd. C 46.87, H 2.46, N 6.83, found: C 47.06, H 2.37, N 6.94, HR-MS (m/z for [M-Cl]<sup>+</sup>): calcd. 580.0671, found: 580.0680. UV-visible spectral data were recorded in DMSO:H<sub>2</sub>O (2:98, v/v) solution where  $\lambda_{\max} = 385$  nm, ( $\epsilon = 0.89 \times 10^4$  M<sup>-1</sup>cm<sup>-1</sup>). <sup>1</sup>H NMR (500 MHz, DMSO-*d*<sub>6</sub>)  $\delta$  9.13 (s, 1H), 9.12–9.10 (m, 2H), 9.09–9.06 (m, 2H), 8.81 (d, *J* = 4.8 Hz, 2H), 8.44–8.35 (m, 2H), 8.23–8.18 (m, 5H), 8.07 (td, *J* = 7.7, 1.8 Hz, 2H), 7.92 (d, *J* = 7.8 Hz, 2H), 7.79 (dd, *J* = 7.7, 5.5 Hz, 2H), 7.66 – 7.59 (m, 7H). <sup>13</sup>C{<sup>1</sup>H} NMR (125 MHz, DMSO-*d*<sub>6</sub>)  $\delta$  198.29, 194.94, 191.46, 161.90, 158.31, 157.63, 156.74, 153.20, 151.16, 149.71, 140.43, 137.42, 135.26, 131.41, 129.84, 129.37, 128.37, 127.96, 126.00, 125.65, 125.43, 124.89, 121.17. IR (cm<sup>-1</sup>): 2017 (s, sh, assym. CO), 1924 (s, sh, assym. CO), 1874 (s, sh, assym. CO), 1423 (m, sh), 851 (s, sh) [m, medium; s, strong; br, broad; sh, sharp, assym., asymmetric].

**Retp2:** Brownish-yellow solid. 88% yield. C<sub>32</sub>H<sub>19</sub>ClN<sub>3</sub>O<sub>3</sub>Re (MW = 715.18 g/mol) calcd. C 53.74, H 2.68, N 5.88, found: C 53.61, H 2.81, N 5.97, HR-MS (m/z for [M-Cl]<sup>+</sup>): calcd. 680.0984, found: 680.0948. UV-visible spectral data were recorded in DMSO:H<sub>2</sub>O (2:98, v/v) solution where  $\lambda_{\max} = 316$  ( $\epsilon = 2.96 \times 10^4$  M<sup>-1</sup>cm<sup>-1</sup>), 371 ( $\epsilon = 1.43 \times 10^4$  M<sup>-1</sup>cm<sup>-1</sup>), 402 ( $\epsilon = 1.40 \times 10^4$  M<sup>-1</sup>cm<sup>-1</sup>). <sup>1</sup>H NMR (500 MHz, DMSO-*d*<sub>6</sub>)  $\delta$  9.15 (d, *J* = 5.5 Hz, 1H), 9.07 (d, *J* = 1.7 Hz, 1H), 8.89 (d, *J* = 8.3 Hz, 1H), 8.86 (s, 1H), 8.78 (d, *J* = 4.8 Hz, 1H), 8.33 – 8.21 (m, 3H), 8.08 – 8.02 (m, 1H), 8.03 – 7.98 (m, 2H), 7.78 (t, *J* = 6.7 Hz, 1H), 7.74 (d, *J* = 8.8 Hz, 1H), 7.65 – 7.57 (m, 4H), 7.57 – 7.47 (m, 2H). <sup>13</sup>C{<sup>1</sup>H} NMR (125 MHz, DMSO-*d*<sub>6</sub>)  $\delta$  197.12,

189.33, 156.18, 154.49, 147.22, 146.06, 143.98, 141.30, 137.08, 135.91, 128.63, 127.94, 127.41, 127.38, 126.89, 125.05, 123.02. IR (cm<sup>-1</sup>): 2020 (s, sh, assym. CO), 1920 (s, sh, assym. CO), 1880 (s, sh, assym. CO), 1537 (m, sh), 1418 (m, sh), 1329 (b, sh) [m, medium; s, strong; br, broad; sh, sharp, assym., asymmetric].

**Retp3:** Yellow solid. 85% yield. C<sub>34</sub>H<sub>19</sub>ClN<sub>3</sub>O<sub>3</sub>Re (MW = 739.20 g/mol) calcd. C 55.25, H 2.59, N 5.68, found: C 55.51, H 2.78, N 5.49, HR-MS (m/z for [M-Cl]<sup>+</sup>): calcd. 704.0984, found: 704.0994. UV-visible spectral data were recorded in DMSO:H<sub>2</sub>O (2:98, v/v) solution where  $\lambda_{\max} = 330$  nm ( $\epsilon = 2.80 \times 10^4$  M<sup>-1</sup>cm<sup>-1</sup>), 370 nm ( $\epsilon = 1.55 \times 10^4$  M<sup>-1</sup>cm<sup>-1</sup>), 435 nm ( $\epsilon = 1.38 \times 10^4$  M<sup>-1</sup>cm<sup>-1</sup>). <sup>1</sup>H NMR (500 MHz, DMSO-*d*<sub>6</sub>)  $\delta$  9.19 (d, *J* = 1.8 Hz, 1H), 9.13 (d, *J* = 5.5 Hz, 1H), 9.00 (d, *J* = 8.3 Hz, 1H), 8.82 (d, *J* = 4.9 Hz, 1H), 8.51 (d, *J* = 8.0 Hz, 1H), 8.42 (dd, *J* = 7.7, 1.1 Hz, 1H), 8.40 – 8.38 (m, 1H), 8.37 – 8.30 (m, 5H), 8.25 (d, *J* = 9.3 Hz, 1H), 8.20 – 8.14 (m, 2H), 8.08 (td, *J* = 7.7, 1.7 Hz, 1H), 8.02 (d, *J* = 7.8 Hz, 1H), 7.80 (t, *J* = 6.7 Hz, 1H), 7.68 – 7.61 (m, 1H). <sup>13</sup>C{<sup>1</sup>H} NMR (125 MHz, DMSO-*d*<sub>6</sub>)  $\delta$  195.02, 191.88, 161.50, 157.30, 153.33, 152.55, 149.92, 140.53, 140.52, 138.13, 137.44, 137.43, 132.37, 131.34, 130.79, 129.61, 127.79, 127.29, 126.23, 125.81, 125.59, 124.50. FT-IR (cm<sup>-1</sup>): 2019 (s, sh, assym. CO), 1916 (s, sh, assym. CO), 1874 (s, sh, assym. CO), 1608 (m, sh), [m, medium; s, strong; br, broad; sh, sharp, assym., asymmetric].

## Methods:

### NMR spectroscopy

<sup>1</sup>H and <sup>13</sup>C NMR spectra were acquired at 293 K Bruker DPX 500 (<sup>1</sup>H = 500 MHz, <sup>13</sup>C = 125 MHz) spectrometers. <sup>1</sup>H and <sup>13</sup>C NMR spectra were recorded at 293 K in DMSO-*d*<sub>6</sub>. All data processing was carried out using MestReNova.

### UV-vis spectra

Agilent Cary 60 UV-Vis spectrophotometer was used with 1 cm path-length quartz cuvettes. Spectra were processed using Origin Pro 2017 software. The UV-vis spectra of **Retp1-Retp3** in DMSO:H<sub>2</sub>O (2:98, v/v) solution were taken at 293 K from 250-700 nm.

### Fluorescence spectra

The fluorescence spectra of complexes **Retp1-Retp3** (10  $\mu$ M) in DMSO:H<sub>2</sub>O (2:98, v/v) solution were recorded with excitation at  $\lambda_{\text{ex}} = 380$  nm in a 1 cm quartz cuvette at room temperature.

### Single Crystal X-ray Crystallography

Single crystals of complexes **Retp1** and **Retp2** were successfully grown in slow diffusion of hexane in methanolic solution of the respective complex. An appropriate single crystal was chosen and securely mounted in a cryo loop using a cryoprotectant oil. Crystal data for **Retp1** and **Retp2** data were collected at 100 K and 293K temperatures respectively, on a Rigaku Oxford diffractometer equipped with a CrysAlis CCD software package using a graphite monochromated MoK $\alpha$  ( $\lambda = 0.71073$  Å) radiation source. X-ray diffraction intensities were collected, integrated, and scaled with APEX4 software. Empirical absorption correction was applied to

the data using a multi-scan method with SADABS programming.<sup>3</sup> The structures were solved by intrinsic phasing with SHELXT<sup>4</sup> and refined by full-matrix least-square methods on F2 using SHELXL using the ShelXle along with the Olex2 interface.<sup>5,6</sup> All non-hydrogen atoms were refined with anisotropic displacement parameters. The hydrogen atoms were introduced at a calculated position. They were treated as riding atoms with an isotropic displacement parameter, C-H = 0.93-0.98 Å with Uiso(H) = 1.5 Ueq for methyl groups, Uiso(H) = 1.2Ueq(C, N) for all other C-H and N-H bonds and O-H = 0.82 Å [Uiso(H) = 1.5Ueq(O)]. ORTEP,<sup>7</sup> Mercury<sup>8</sup>, and publCIF<sup>9</sup> were used for molecular graphics, validation and to prepare material for publication. Details of crystal data collections and data refinement parameters are given in **Table S1**. The complete crystallographic information file (CIF) for **Retp1** and **Retp2** was deposited in the Cambridge Crystallographic Data Centre (CCDC: 2333274 (**Retp1**); 2333273 (**Retp2**)).

### DFT Calculation

The complexes, **Retp1-Retp3** were studied in their neutral form by Density Functional Theory (DFT) using the Gaussian 16 quantum chemistry package, revision A.03.<sup>10</sup> We have used the LANL2DZ basis set for Re and 6-31g\* for all other atoms with the B3LYP function for geometry optimization in a vacuum. Thereafter, ground state (S<sub>0</sub>), first singlet excited state (S<sub>1</sub>), and first excited triplet state (T<sub>1</sub>) geometry optimizations were carried out using B3LYP, TD-B3LYP, and UB3LYP respectively coupled to LANL2DZ/6-31g\* basis set. All the calculations are carried out in water solvent and implicit CPCM solvation model as implemented in the package. The optimized ground state and T<sub>1</sub> structures were confirmed to local minima at the same computational level. The plots were drawn using GaussView 5.0.

### <sup>1</sup>O<sub>2</sub> generation

The <sup>1</sup>O<sub>2</sub> generation was measured using probe 9,10-diphenyl anthracene (DPA) upon light irradiation. In brief, a DMSO:PBS solution (2:98 v/v) containing 10 μM of **Retp1-Retp3** and 0.3 μg/mL of DPA was monitored by UV-vis spectroscopy after different durations of light exposure (400-700 nm, 10 J cm<sup>-2</sup>). The absorbance at 378 nm was monitored for <sup>1</sup>O<sub>2</sub> generation.

### Detection of OH<sup>•</sup> generation

The production of hydroxyl radical (OH<sup>•</sup>) in solution was detected using Methylene Blue (MB) as an OH<sup>•</sup> probe. The reaction between 10 μM of **Retp1-Retp3** and 5 μg/mL methylene blue (MB) in DMSO:PBS (2:98, v/v) solution was monitored by UV-vis spectroscopy after different durations of visible light (400-700 nm, 10 J cm<sup>-2</sup>) irradiation.

### NADH Oxidation

Reactions between **Retp1-Retp3** (15 μM) and NADH (250 μM) in DMSO:PBS (2:98, v/v) solution were monitored by UV-Vis. spectroscopy at ambient temperature in the dark or on irradiation with visible light (400-700 nm, 10 J cm<sup>-2</sup>). The turnover number of catalysis was calculated using the following equations:

$$[\text{NAD}^+] = [\text{Abs}(339 \text{ nm})_{\text{initial}} - \text{Abs}(339 \text{ nm})_{\text{final}}] / \text{Abs}(339 \text{ nm})_{\text{initial}} * [\text{NADH}]$$

$$\text{Turnover number (TON)} = [\text{NAD}^+]/[\text{Catalyst}]$$

$$\text{Turnover frequency (TOF)} = \text{Turnover number}/\text{time (h)}$$

### Detection of H<sub>2</sub>O<sub>2</sub> generation

During the reaction of **Retp3** (15  $\mu\text{M}$ ) with NADH (250  $\mu\text{M}$ ) in the DMSO:PBS (2:98, v/v) solution at ambient temperature in the dark or after light (400-700 nm, 10 J cm<sup>-2</sup>) irradiation for 20 min, H<sub>2</sub>O<sub>2</sub> was detected by Quantofix peroxide test sticks. The H<sub>2</sub>O<sub>2</sub> generation level in the solution can be co-related to the color change from white to blue (of the test sticks), indicating 0-25 mg/L amount of H<sub>2</sub>O<sub>2</sub>.

### Cell culture and cell assays:

#### MTT assay

A cytotoxicity assessment was conducted on A549 cells (human lung adenocarcinoma cell line), HeLa cells (a human cervical cancer cell line), and Beas-2B cells (non-tumorigenic human bronchial epithelial cell line) to evaluate the cytotoxic impact of **Retp1-Retp3**. The cells were cultured in a mixture of 10% FBS and DMEM at 37 °C in a 5% CO<sub>2</sub> environment. In 96-well plates, approximately 8000 cells of each type (A549, HeLa, and Beas-2B) were seeded. The cells were subjected to a variety of concentrations, commencing with an initial concentration of 50  $\mu\text{M}$ , and subsequently, a serial dilution was performed, reducing the concentration to as low as 0.195  $\mu\text{M}$  for **Retp1-Retp3**. This treatment was carried out in a medium consisting of 1% DMSO and DMEM for a duration of 4 h, all while being conducted in a light-restricted environment. Following the removal of the compound-containing medium, Dulbecco's phosphate-buffered saline (DPBS) was used to wash the cells. Subsequently, one set of cells was exposed to visible light for 1 h with a wavelength of 400-700 nm and a dose of 10 J cm<sup>-2</sup>. After the light treatment, fresh DMEM media were added to the cells. The other set of cells was maintained in darkness with the fresh DMEM medium. Both sets of cells were then incubated in the dark for an additional 43 h, resulting in a total incubation period of 48 h. The IC<sub>50</sub> values were determined using GraphPad Prism 8 software.

#### Confocal microscopy

In aseptic conditions, approximately  $1 \times 10^5$  A549 cells were seeded onto glass-bottomed petri dishes and allowed to adhere for 24 h in a CO<sub>2</sub> incubator. Subsequently, a solution of **Retp3** at a concentration of 30  $\mu\text{M}$  was introduced into the glass-bottom dishes, and the cells were incubated at 37 °C for 4 h. Following this incubation period, the cells were thoroughly washed with DPBS. To label specific organelles, the cells were then treated with MitoTracker red at 250 nM. Finally, triple rinsing with PBS was performed, and images were acquired using an oil immersion lens with a magnification of 63X. Image acquisition and processing were carried out utilizing ZEN 3.3 (blue edition software).



### **DCFDA assay**

Glass bottom dishes were seeded with  $1 \times 10^5$  cells and allowed to adhere for 24 h within an incubator. Subsequently, the cells were treated with a complex **Retp3** solution (2  $\mu\text{M}$ ) and incubated for 4 h in darkness at 37°C in a 5% CO<sub>2</sub> environment. Following treatment, the cells underwent triple washing with PBS buffer and were then stained with DCFDA (5  $\mu\text{M}$ ) for 30 min at room temperature in darkness. A division was made: one batch of cells was exposed to photo-irradiation spanning from 400 to 700 nm at a dosage of 10 J cm<sup>-2</sup>, while the other batch was kept in darkness. After that, confocal images were recorded with 10X magnification. Images were processed by using LASX software.

### **JC-1 assay**

Approximately  $1 \times 10^5$  A549 cells were seeded into 12-well plates and given a 24 h window to adhere. Subsequently, the cells were treated with the **Retp3** at a concentration of 2  $\mu\text{M}$  and allowed to incubate in darkness at 37°C for 4 h. Following this incubation period, the cells were subjected to a PBS buffer wash. After that, one group of cells was exposed to visible light with 10 J cm<sup>-2</sup> light dose, while the other group remained in darkness. Cells were then incubated for 30 minutes post-irradiation. To visualize changes, the cells were then stained using JC-1 dye, and confocal images were captured at a 63X magnification. The acquired images were processed using ZEN 3.3 (blue edition) software.

### **3D MCTs**

To culture the spheroids, around 8000 A549 cells were suspended in 150  $\mu\text{L}$  of media and seeded into each well of an ultra-low attachment 96 well plate. Multicellular tumor spheroids were formed over the course of three days. These spheroids were exposed to **Retp3** for 8 hours at a concentration of 30  $\mu\text{M}$  in a light-free environment. Utilizing 380 nm excitation, Z-stack confocal luminescence images of the MCTs were captured after incubation, with emission signals recorded within the range of 440 to 480 nm.

**Tables:****Table S1.** Crystal data parameters and refinement details of **Retp1** and **Retp2**.

| Entry                                  | Retp1  | Retp2  |
|--|--|--|
| Empirical formula                      | C <sub>24</sub> H <sub>15</sub> ClN <sub>3</sub> O <sub>3</sub> Re | C <sub>34.33</sub> H <sub>21.67</sub> ClN <sub>3</sub> O <sub>3</sub> Re |
| Formula weight                         | 615.04   | 745.83   |
| Temperature/K                          | 100.0  | 293  |
| Crystal system                         | monoclinic   | triclinic  |
| Space group                            | P2 <sub>1</sub> /c   | P-1  |
| a/Å                                    | 11.5938(2)   | 7.7233(2)  |
| b/Å                                    | 11.5936(3)   | 13.4308(4)   |
| c/Å                                    | 15.8191(3)   | 14.3953(5)   |
| $\alpha$ /°                            | 90   | 89.027(2)  |
| $\beta$ /°                             | 101.8760(10)   | 82.586(3)  |
| $\gamma$ /°                            | 90   | 79.332(2)  |
| Volume/Å <sup>3</sup>                  | 2080.79(8)   | 1455.11(8)   |
| Z                                      | 4  | 2  |
| $\rho_{\text{calc}}/\text{cm}^3$       | 1.963  | 1.6322   |
| $\mu/\text{mm}^{-1}$                   | 6.001  | 4.308  |
| F(000)                                 | 1184.0   | 694.9  |
| Crystal size/mm <sup>3</sup>           | 0.02 × 0.01 × 0.01   | 0.03 × 0.02 × 0.01   |
| Radiation                              | MoK $\alpha$ ( $\lambda$ = 0.71073)                                | Mo K $\alpha$ ( $\lambda$ = 0.71073)                                     |
| 2 $\Theta$ range for data collection/° | 4.39 to 56.622   | 5.41 to 50   |
| Index ranges                           | -15 ≤ h ≤ 15, -15 ≤ k ≤ 15,<br>-21 ≤ l ≤ 21                        | -8 ≤ h ≤ 9, -15 ≤ k ≤ 15, -<br>17 ≤ l ≤ 17                               |
| Reflections collected                  | 22113  | 21186  |
| Independent reflections                | 5171 [R <sub>int</sub> = 0.0259,<br>R <sub>sigma</sub> = 0.0219]   | 5030 [R <sub>int</sub> = 0.0708,<br>R <sub>sigma</sub> = 0.0884]         |

|  |                                  |                                  |
|--|----------------------------------|----------------------------------|
| Data/restraints/parameters                     | 5171/0/289                       | 5030/0/331                       |
| Goodness-of-fit on $F^2$                       | 1.032                            | 1.044                            |
| Final R indexes [ $I \geq 2\sigma(I)$ ]        | $R_1 = 0.0160$ , $wR_2 = 0.0324$ | $R_1 = 0.0479$ , $wR_2 = 0.0941$ |
| Final R indexes [all data]                     | $R_1 = 0.0193$ , $wR_2 = 0.0334$ | $R_1 = 0.0713$ , $wR_2 = 0.1019$ |
| Largest diff. peak/hole / $e \text{ \AA}^{-3}$ | 0.50/-0.45                       | 1.10/-0.71                       |
| CCDC   | <b>2333274</b>                   | <b>2333273</b>                   |

**Table S2:** Selected bond lengths ( $\text{\AA}$ ) and bond angles ( $^\circ$ ) of **Retp1** and **Retp2**.

| Bond Lengths    |            |            | Bond Angles |            |           |
|-----------------|------------|------------|-------------|------------|-----------|
| Bond(s)         | Retp1      | Retp2      | Angle(s)    | Retp1      | Retp2     |
| Re-Cl           | 2.4873(5)  | 2.4784(18) | Cl-Re-N1    | 84.14(4)   | 83.67(15) |
| Re-C1           | 1.936(2)   | 1.891(10)  | Cl-Re-N2    | 82.99(4)   | 80.44(14) |
| Re-C2           | 1.902(2)   | 1.881(8)   | Cl-Re-C1    | 91.52(6)   | 89.7(2)   |
| Re-C3           | 1.908(2)   | 1.917(9)   | Cl-Re-C2    | 93.86(6)   | 93.5(2)   |
| Re-N1           | 2.1706(17) | 2.166(6)   | Cl-Re-C3    | 178.78(6)  | 177.8(2)  |
| Re-N2           | 2.2211(16) | 2.221(5)   | N1-Re-N2    | 74.45(6)   | 73.7(2)   |
| C7-C8           | 1.487(3)   | 1.484(10)  | C1-Re-N2    | 101.36(7)  | 100.4(3)  |
| Dihedral Angles |            |            | N1-Re-C1    | 174.28(7)  | 171.8(3)  |
| Angle(s)        | Retp1      | Retp2      | N1-Re-C3    | 95.85(8)   | 94.9(3)   |
| C6-C7-C8-C9     | -165.79    | -90.21     | N2-Re-C2    | 170.33(8)  | 169.6(3)  |
| C6-C7-C8-C10    | 13.71      | 88.07      | N2-Re-C3    | 95.83(7)   | 97.6(3)   |
| N2-C12-C13-N3   | -48.94     | -44.48     | N2-C5-C4    | 115.40(17) | 116.4(6)  |
| C11-C12-C13-N3  | 127.23     | 131.17     | N2-C12-C13  | 119.21(17) | 120.7(6)  |

**Table S3.** Energy (eV) of the lowest vertical 10 singlet–singlet ( $S_0 \rightarrow S_n$ ;  $n = 1$  to 10) transitions for the complexes computed at the TD-B3LYP /LANL2DZ/6-31g\* level of theory in water. The oscillator strengths are indicated in parentheses.

|              | S <sub>1</sub>          | S <sub>2</sub>          | S <sub>3</sub>   | S <sub>4</sub>   | S <sub>5</sub>   | S <sub>6</sub>   | S <sub>7</sub>   | S <sub>8</sub>    | S <sub>9</sub>   | S <sub>10</sub>  |
|--------------|-------------------------|-------------------------|------------------|------------------|------------------|------------------|------------------|-------------------|------------------|------------------|
| <b>Retp1</b> | <b>2.93</b><br>(0.0079) | <b>3.15</b><br>(0.1175) | 3.34<br>(0.0053) | 3.71<br>(0.0017) | 3.85<br>(0.0122) | 3.91<br>(0.0076) | 3.96<br>(0.2465) | 4.08<br>(0.1023)  | 4.10<br>(0.0104) | 4.13<br>(0.0007) |
| <b>Retp2</b> | <b>2.49</b><br>(0.0340) | 2.95<br>(0.0079)        | 3.08<br>(0.1226) | 3.18<br>(0.0839) | 3.25<br>(0.0360) | 3.35<br>(0.0035) | 3.68<br>(0.0071) | 3.70<br>(0.0003)  | 3.76<br>(0.0177) | 3.84<br>(0.0002) |
| <b>Retp3</b> | <b>2.64</b><br>(0.2466) | 2.92<br>(0.0108)        | 3.16<br>(0.0237) | 3.27<br>(0.0205) | 3.33<br>(0.0038) | 3.50<br>(0.0698) | 3.64<br>(0.2227) | 3.69<br>(0.00325) | 3.81<br>(0.0138) | 3.85<br>(0.0192) |

**Table S4.** Energy (eV) of the lowest vertical 10 singlet–triplet ( $S_0 \rightarrow T_n$ ;  $n = 1$  to 10) transitions for the complexes computed at the TD-B3LYP /LANL2DZ/6-31g\* level of theory in water.<sup>a</sup>

|              | T <sub>1</sub> | T <sub>2</sub> | T <sub>3</sub> | T <sub>4</sub> | T <sub>5</sub> | T <sub>6</sub> | T <sub>7</sub> | T <sub>8</sub> | T <sub>9</sub> | T <sub>10</sub> |
|--------------|----------------|----------------|----------------|----------------|----------------|----------------|----------------|----------------|----------------|-----------------|
| <b>Retp1</b> | 2.78           | 2.92           | 3.06           | 3.30           | 3.31           | 3.53           | 3.64           | 3.75           | 3.79           | 3.86            |
| <b>Retp2</b> | 1.75           | 2.46           | 2.81           | 2.99           | 3.07           | 3.11           | 3.29           | 3.31           | 3.46           | 3.48            |
| <b>Retp3</b> | 1.99           | 2.62           | 2.80           | 2.99           | 3.06           | 3.22           | 3.28           | 3.30           | 3.50           | 3.51            |

<sup>a</sup>Calculating the oscillator strengths is beyond the scope of the theory used.

**Figures:**

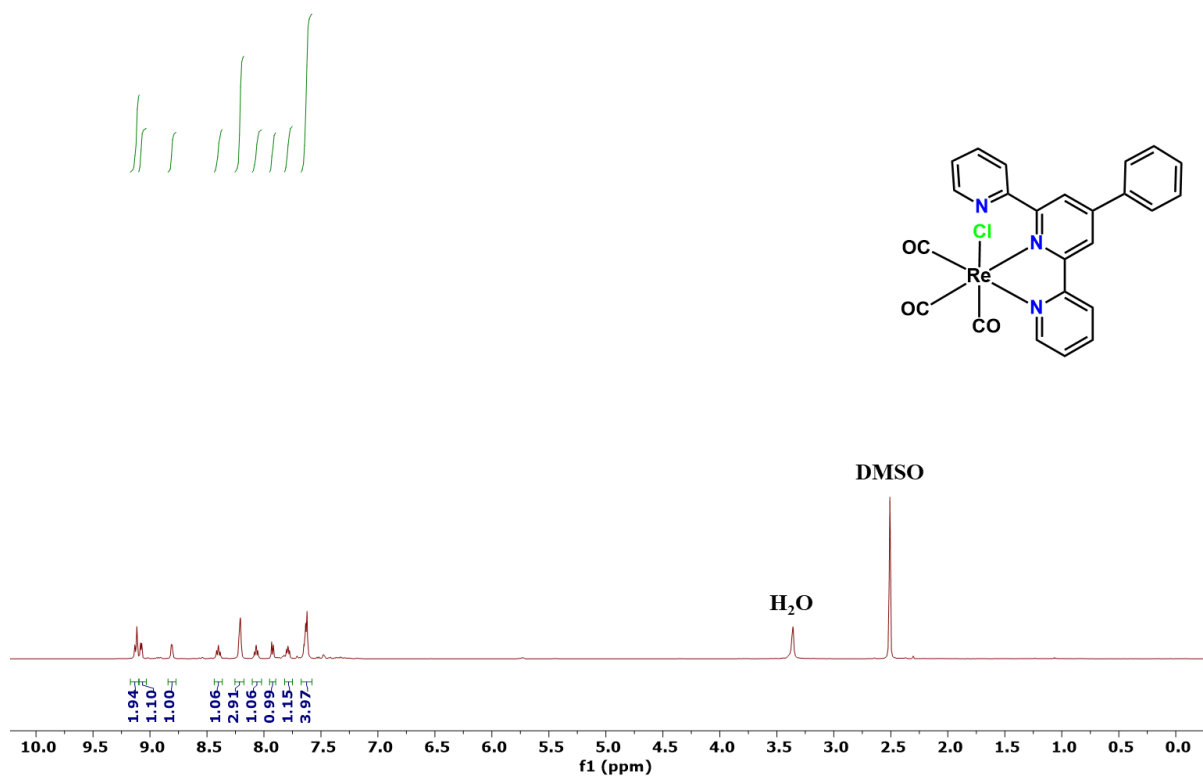


**Figure S1:** <sup>1</sup>H NMR of Retp1 in DMSO-d<sub>6</sub> (500 MHz).

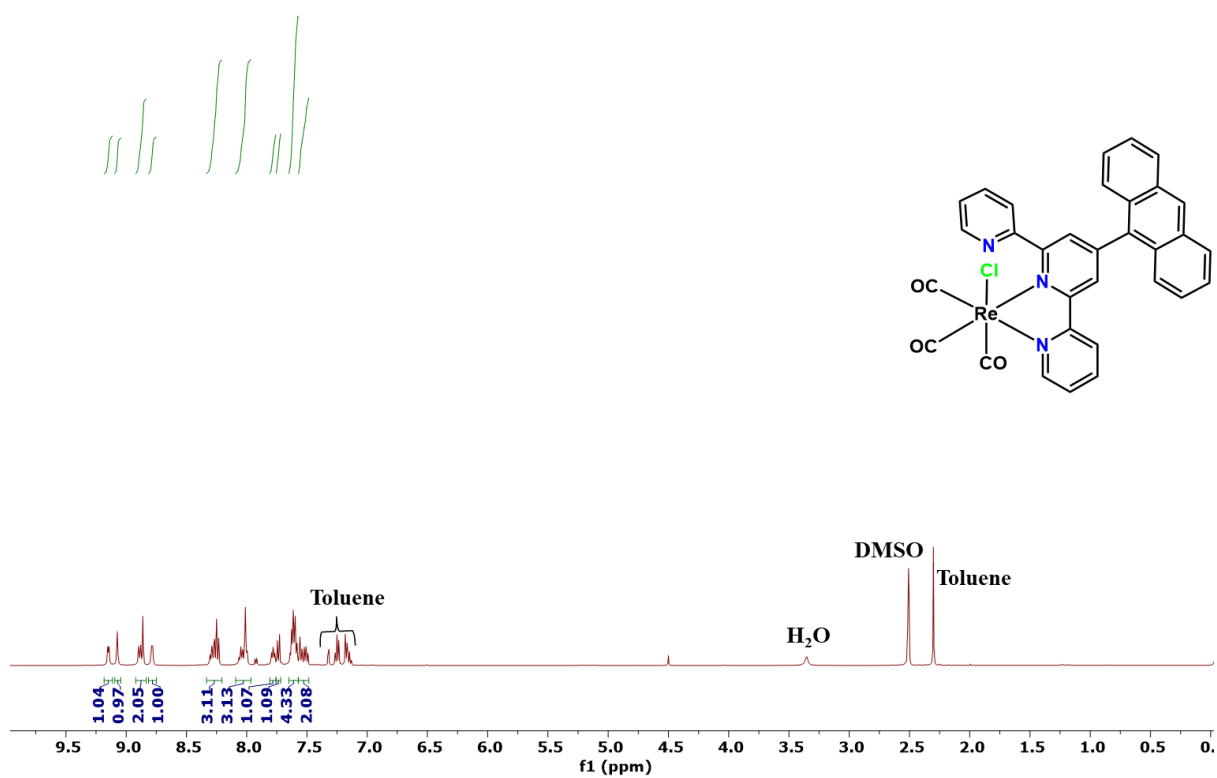


Figure S2: <sup>1</sup>H NMR of Retp2 in DMSO-d<sub>6</sub> (500 MHz).

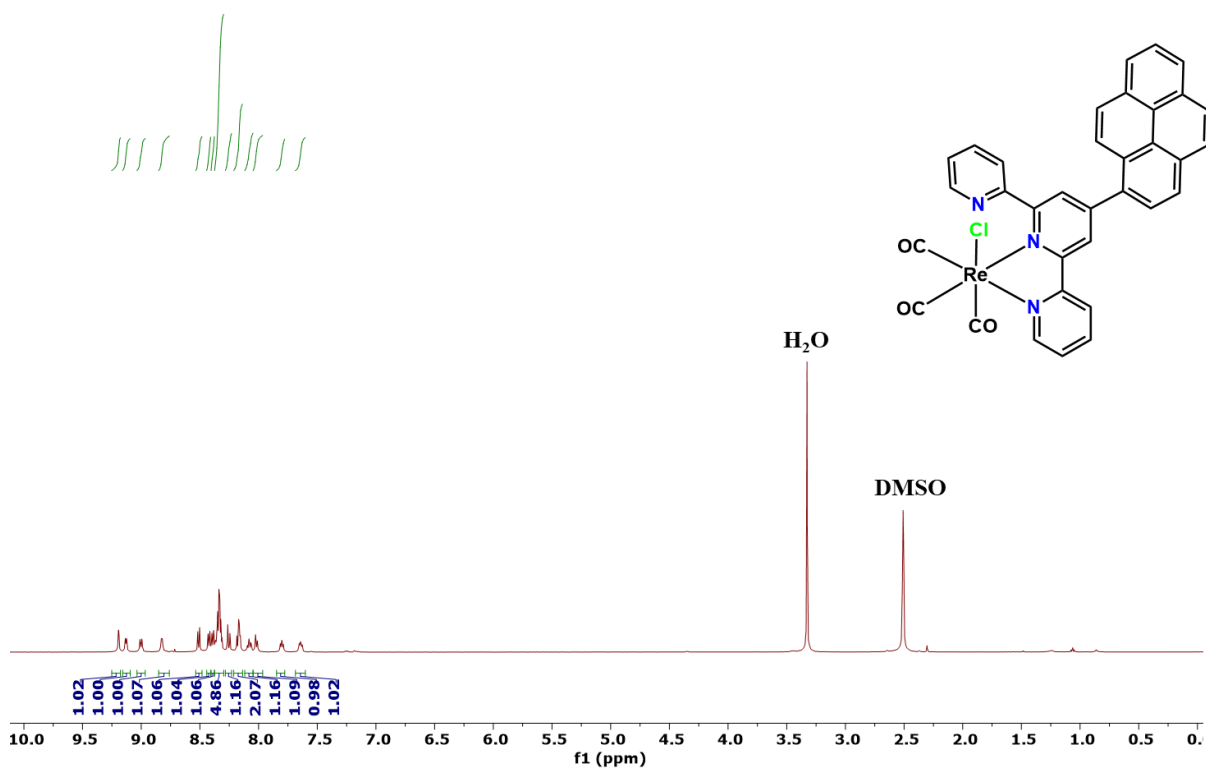
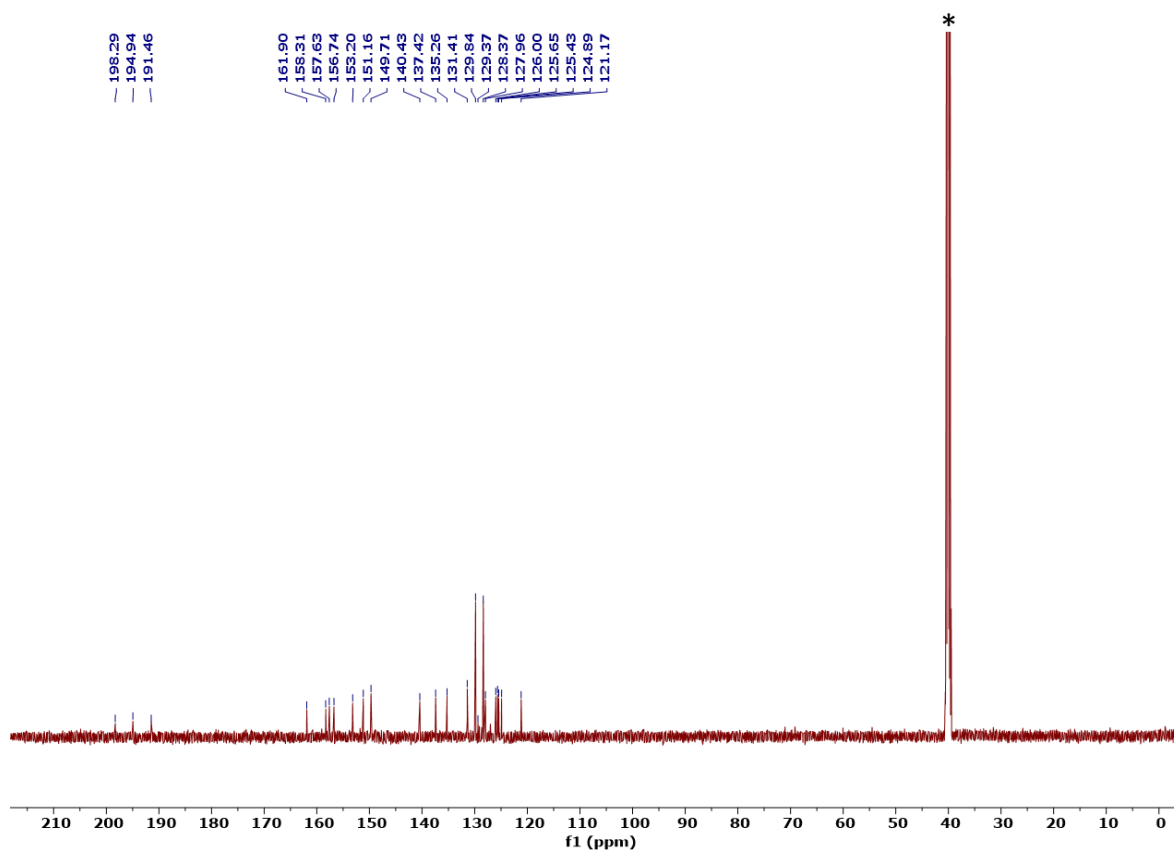
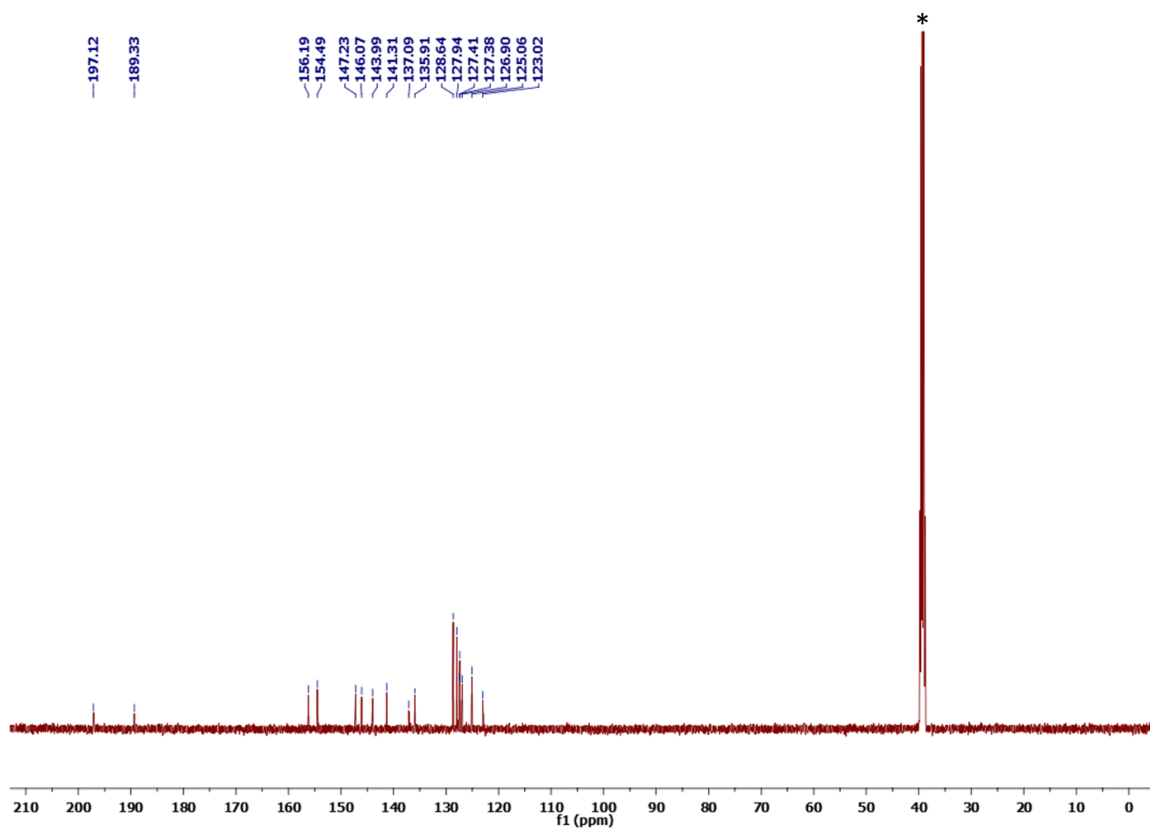


Figure S3: <sup>1</sup>H NMR of Retp3 in DMSO-d<sub>6</sub> (500 MHz).



**Figure S4:**  $^{13}\text{C}\{^1\text{H}\}$  NMR of **Retp1** in  $\text{DMSO-d}_6$  (125 MHz). (Residual solvent peaks: \*  $\text{DMSO-d}_6$ )



**Figure S5:**  $^{13}\text{C}\{^1\text{H}\}$  of **Retp2** in  $\text{DMSO-d}_6$  (125 MHz). (Residual solvent peaks: \*  $\text{DMSO-d}_6$ )

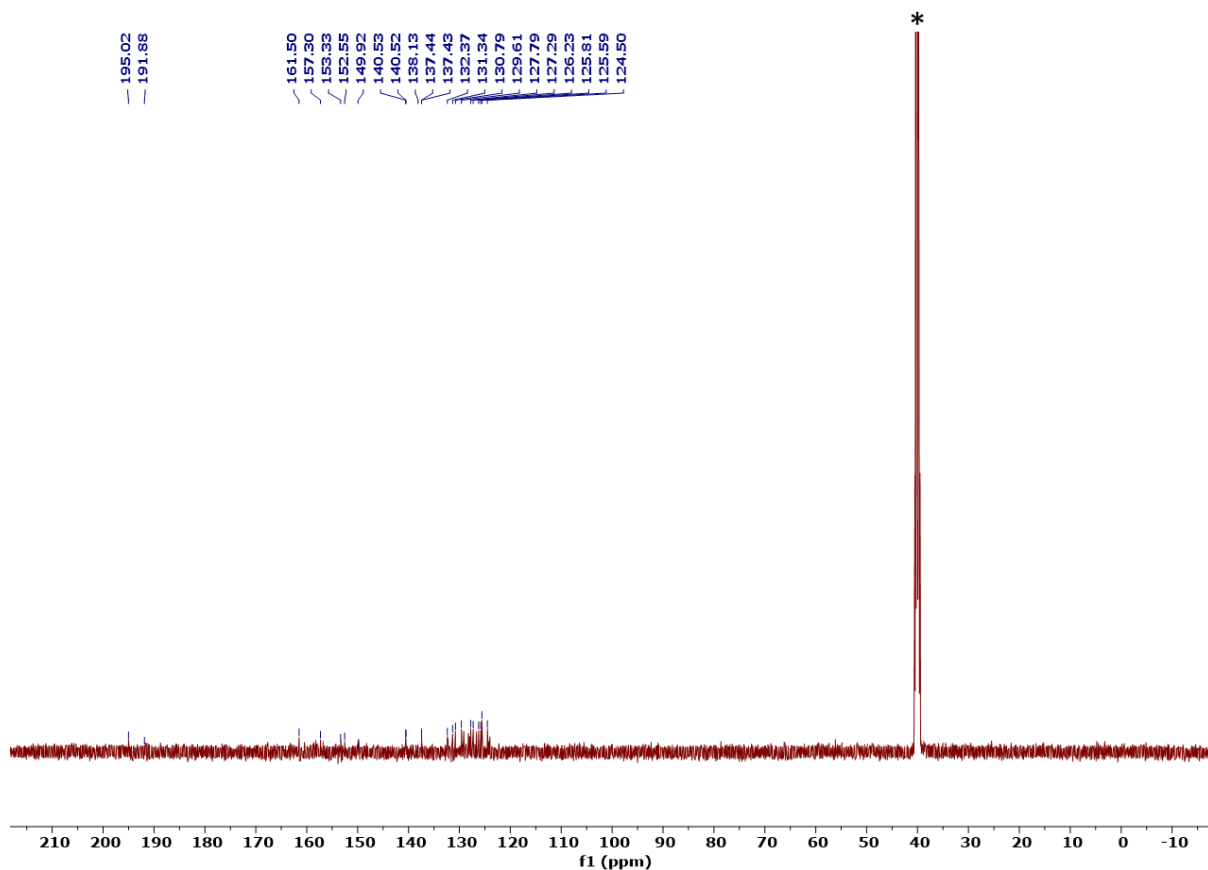


**Figure S6:**  $^{13}\text{C}\{^1\text{H}\}$  NMR of **Retp3** in DMSO- $\text{d}_6$  (125 MHz). (Residual solvent peaks: \*DMSO- $\text{d}_6$ )

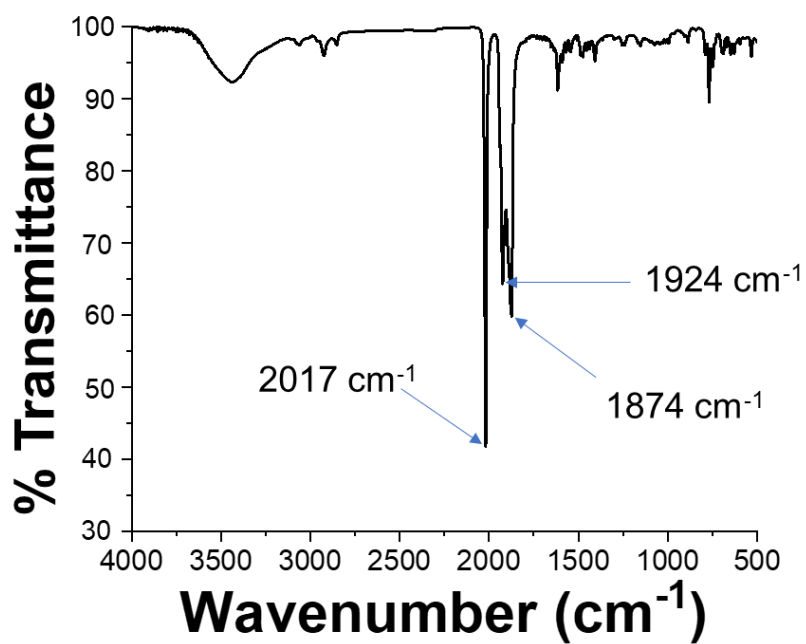


**Figure S7:** IR spectra of **Retp1**.

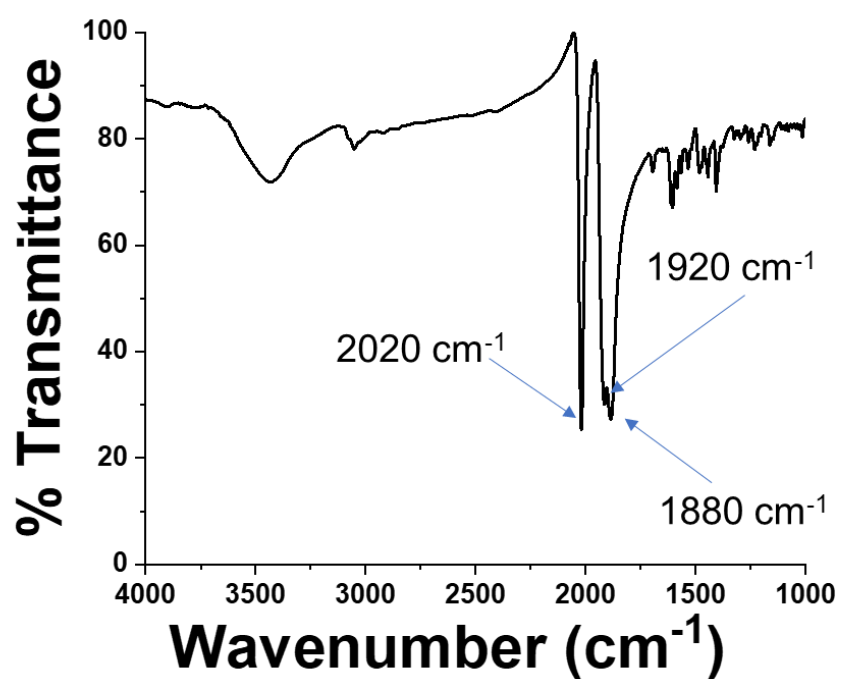


Figure S8: IR spectra of **Retp2**.

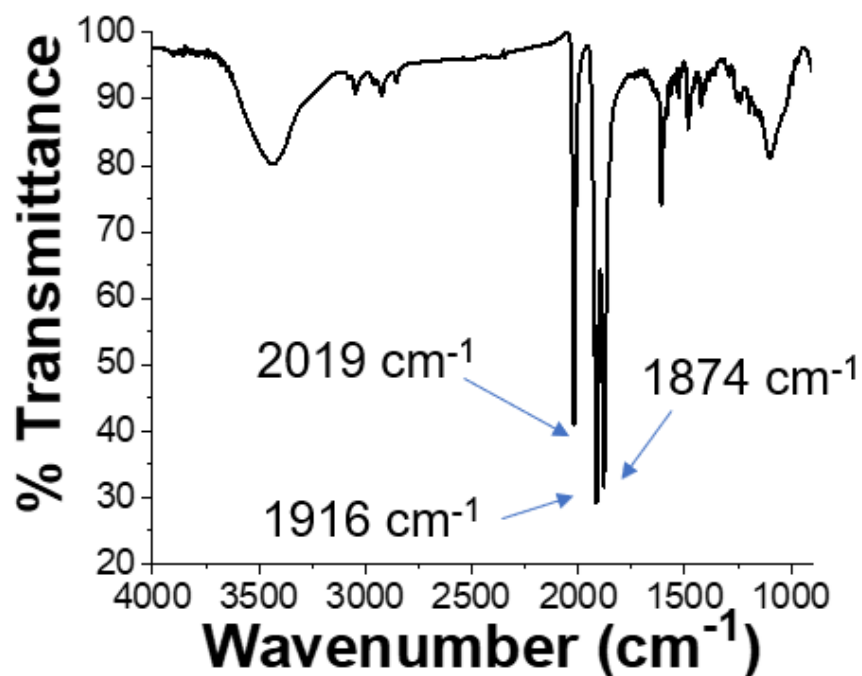
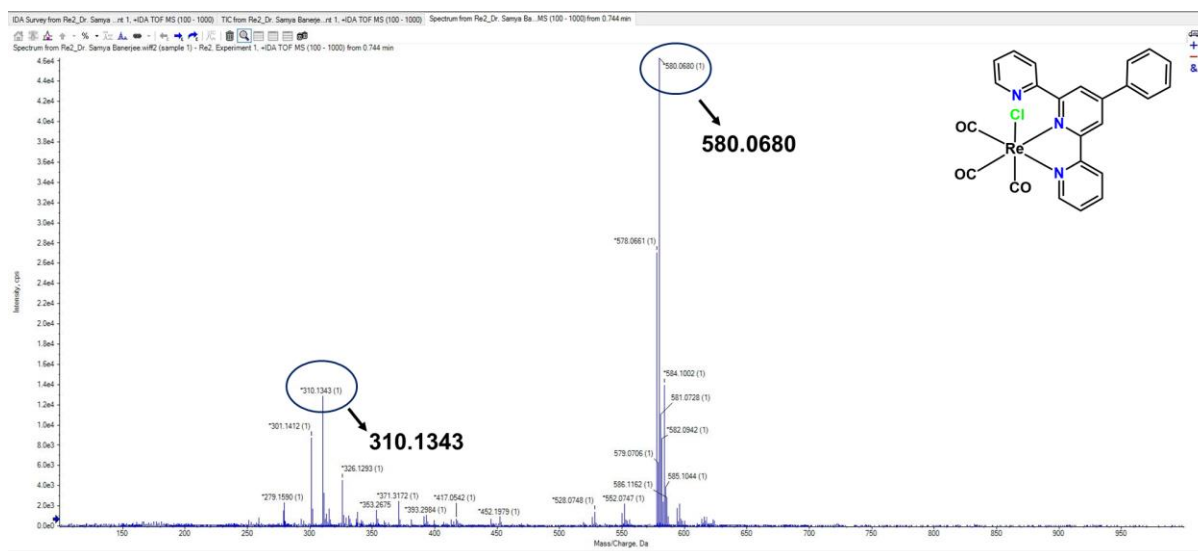
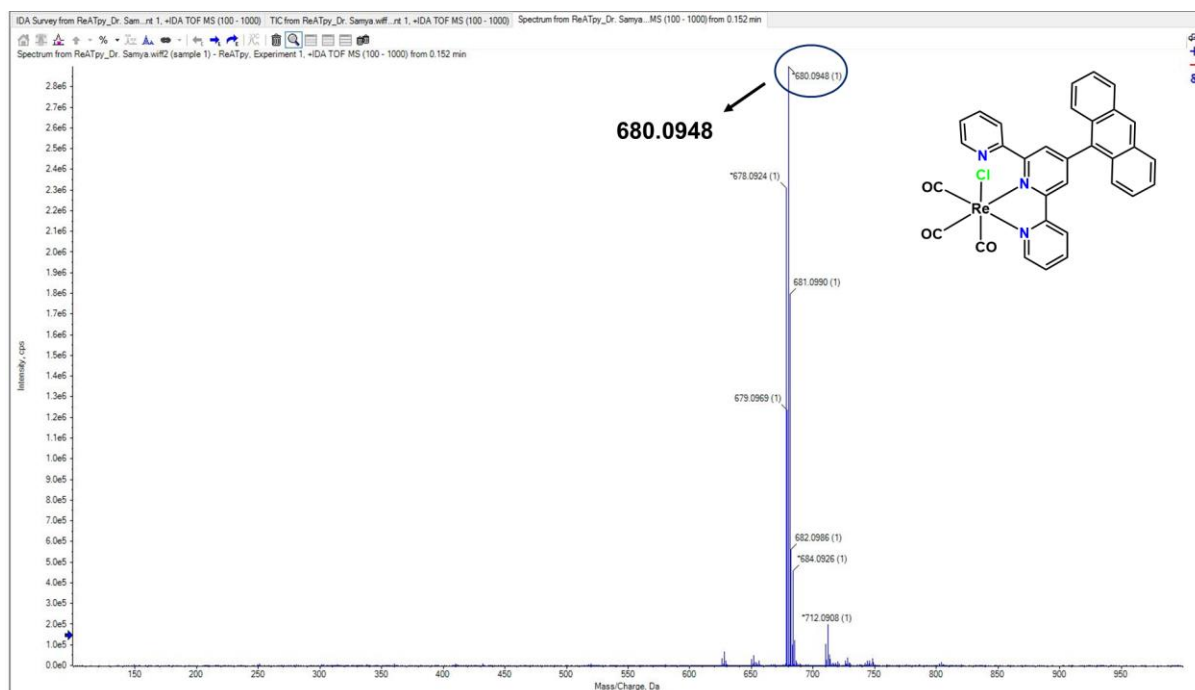


Figure S9: IR spectra of **Retp3**.





**Figure S10:** HRMS of **Retp1** in CH<sub>3</sub>CN. The calculated m/z value for: [M-Cl]<sup>+</sup> = 580.0671, [tp1+H]<sup>+</sup> = 310.1344



**Figure S11:** HRMS of **Retp2** in CH<sub>3</sub>CN. The calculated m/z value for [M-Cl]<sup>+</sup> = 680.0984

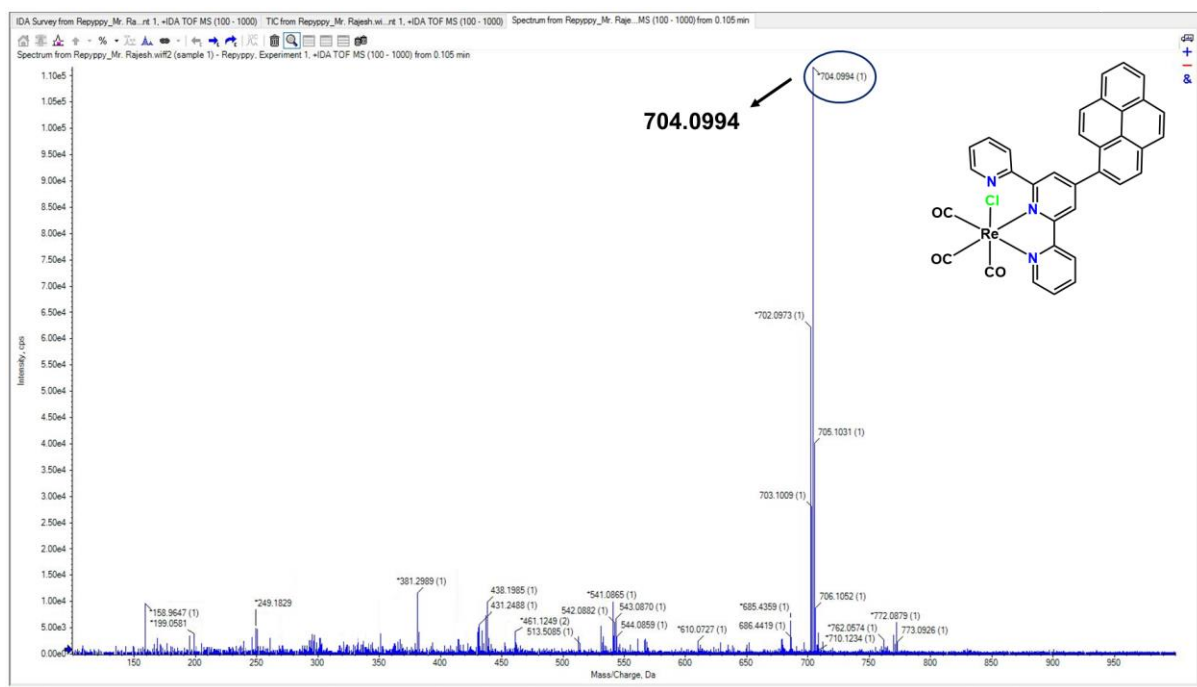


**Figure S12:** HRMS of **Retp3** in  $\text{CH}_3\text{CN}$ . The calculated  $m/z$  value for  $[\text{M}-\text{Cl}]^+ = 704.0984$

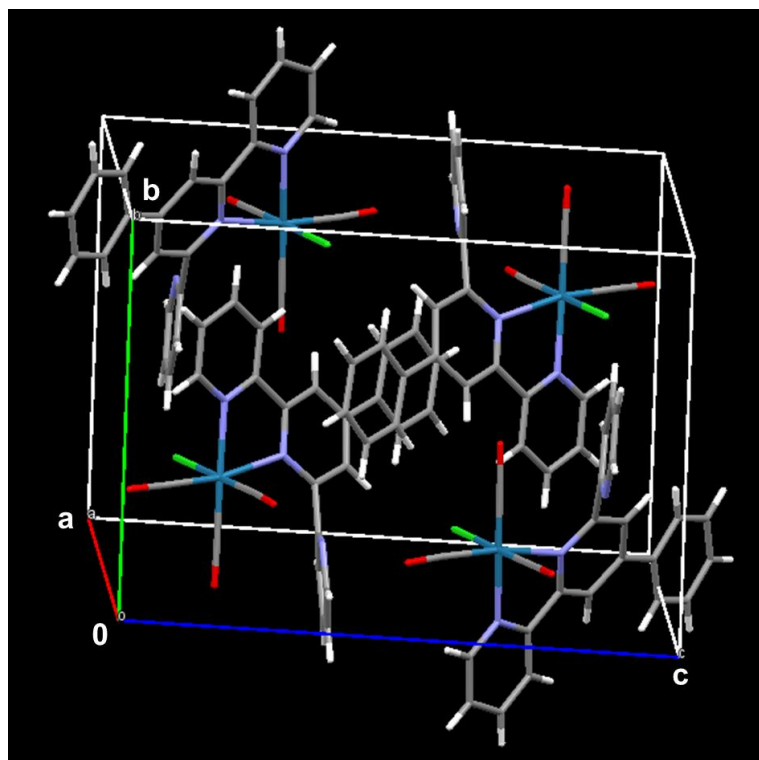


**Figure S13:** Unit cell packing of **Retp1**, the plot is drawn using mercury 3.8 software.

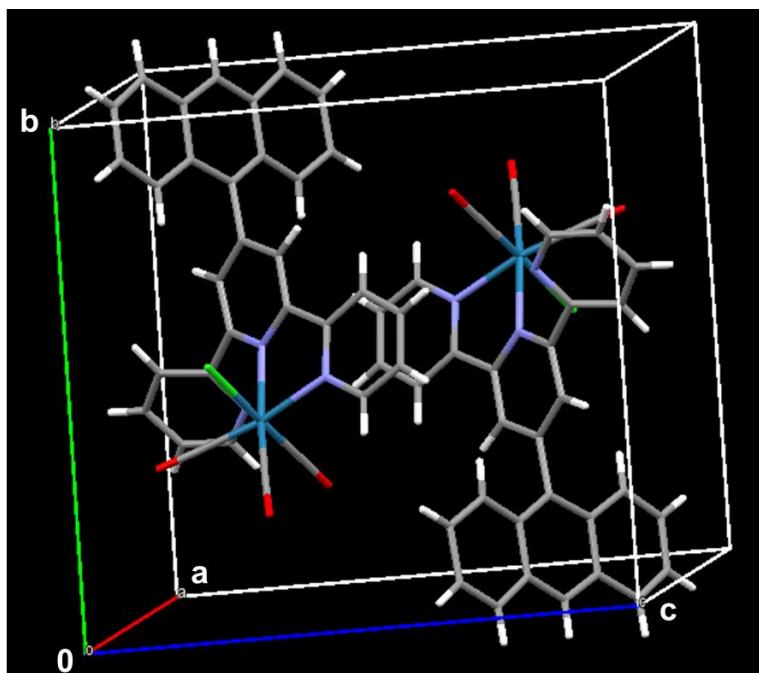


**Figure S14:** Unit cell packing of **Retp2**, the plot is drawn using mercury 3.8 software.

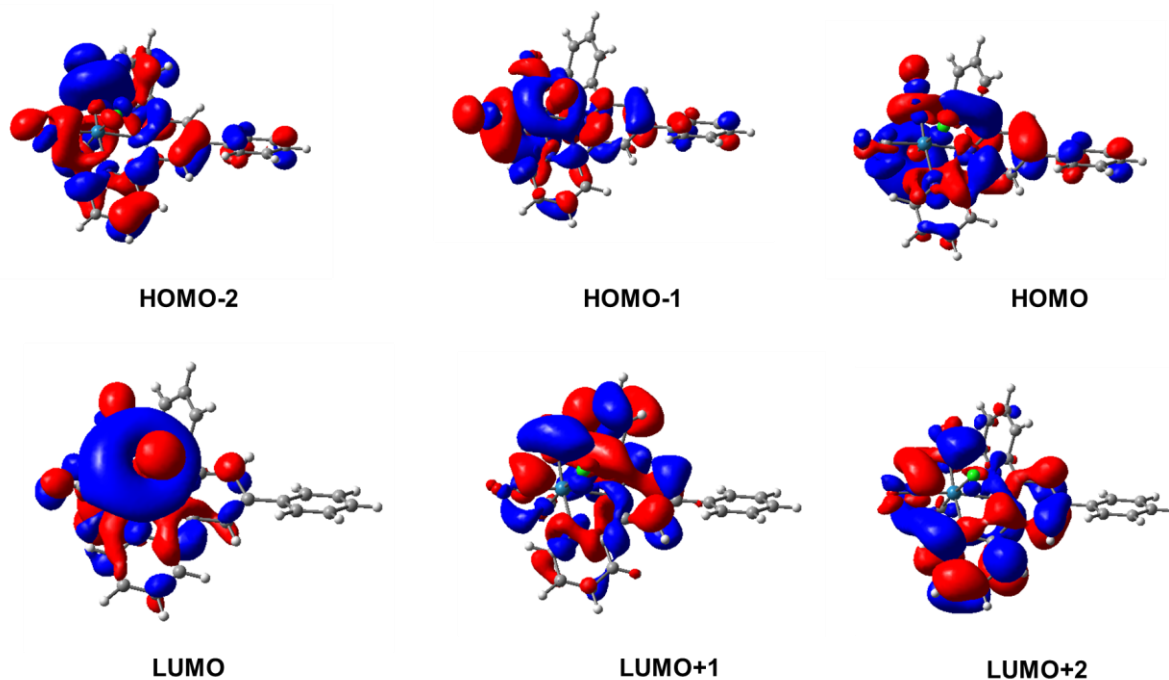


**Figure S15:** Spatial plots of selected frontier orbitals of the DFT optimized ground state of **Retp1**.

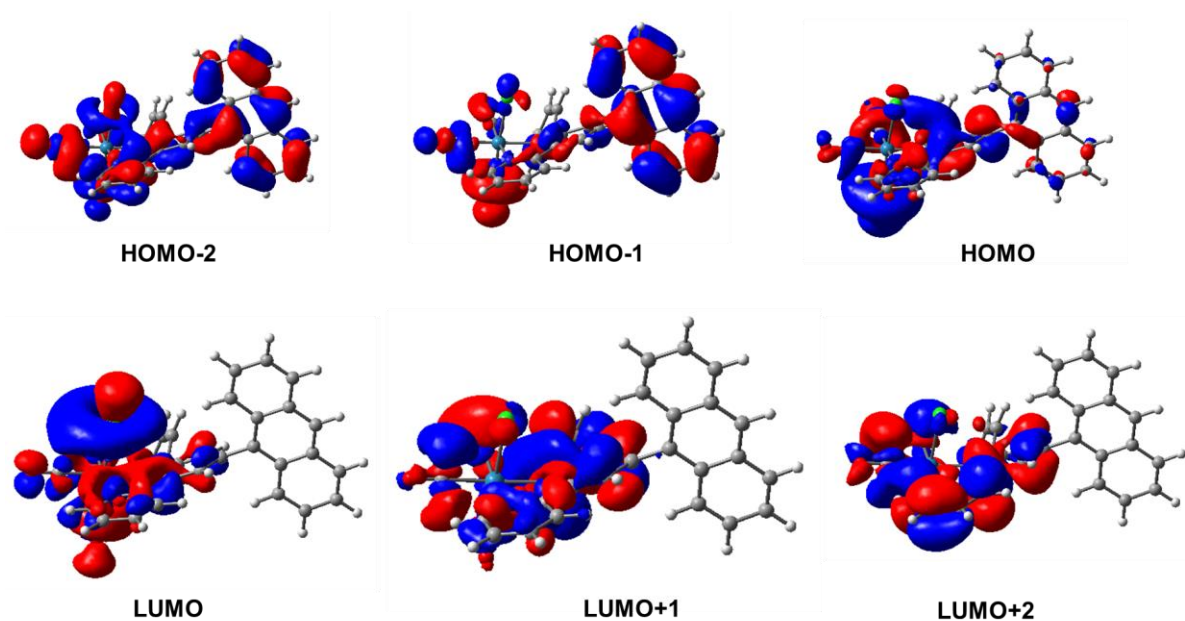


**Figure S16:** Spatial plots of selected frontier orbitals of the DFT optimized ground state of **Retp2**.

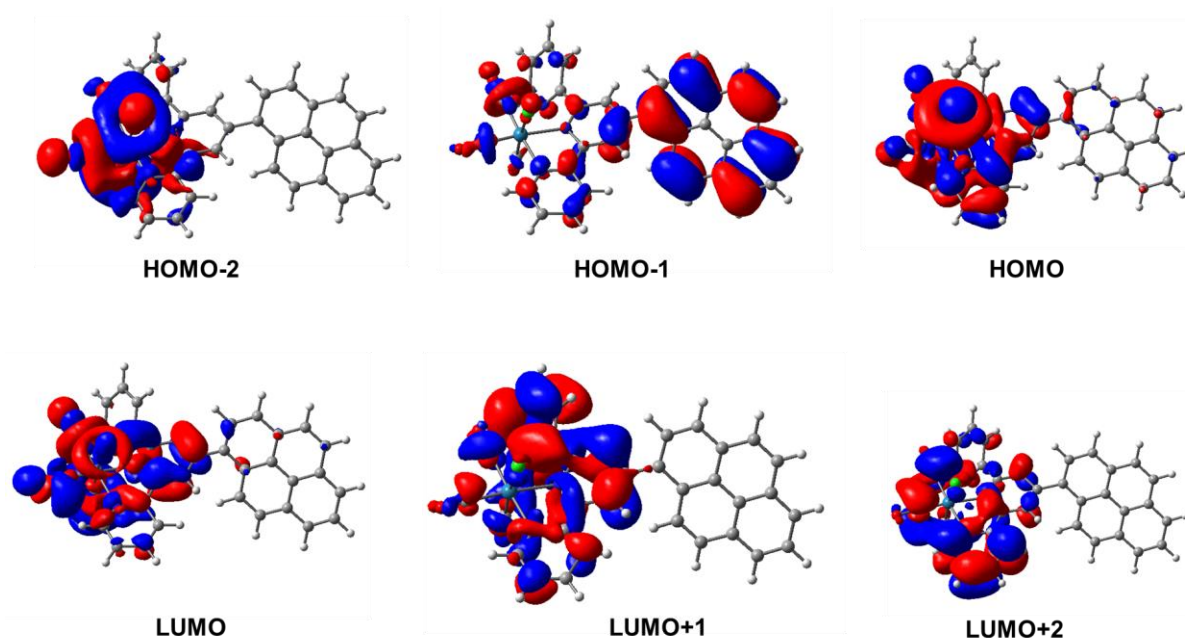


**Figure S17:** Spatial plots of selected frontier orbitals of the DFT optimized ground state of **Retp3**.

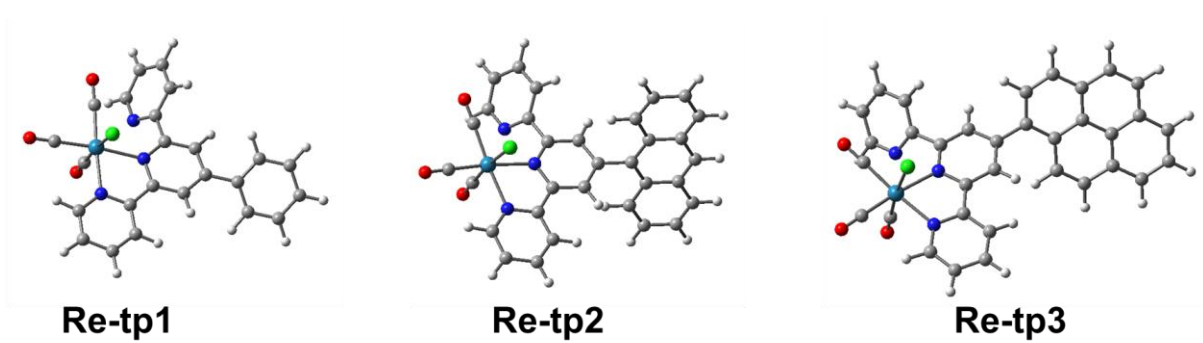


**Figure S18:** Optimized structures of the complexes, **Retp1-Retp3**, in the singlet state (S1).

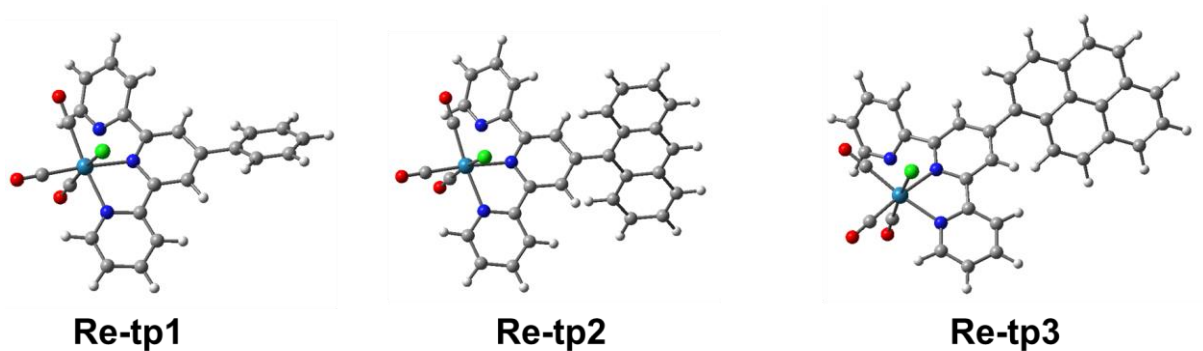


**Figure S19:** Optimized structures of the complexes, **Retp1-Retp3**, in the triplet state (T1).

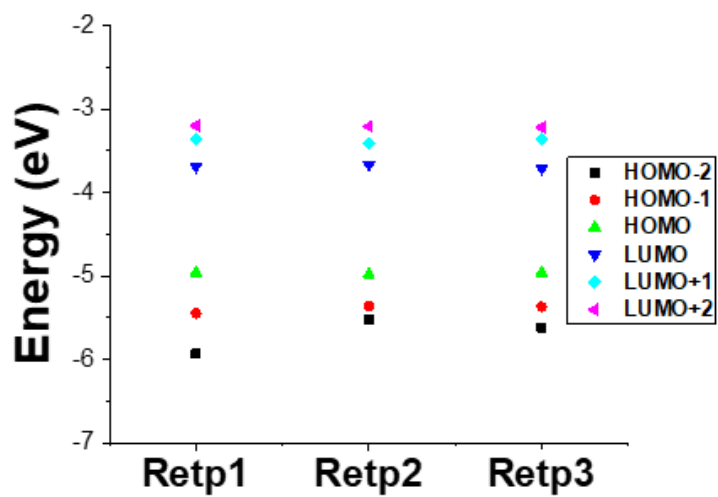


**Figure S20:** Calculated frontier orbital energies of ground states of **Retp1-Retp3**.

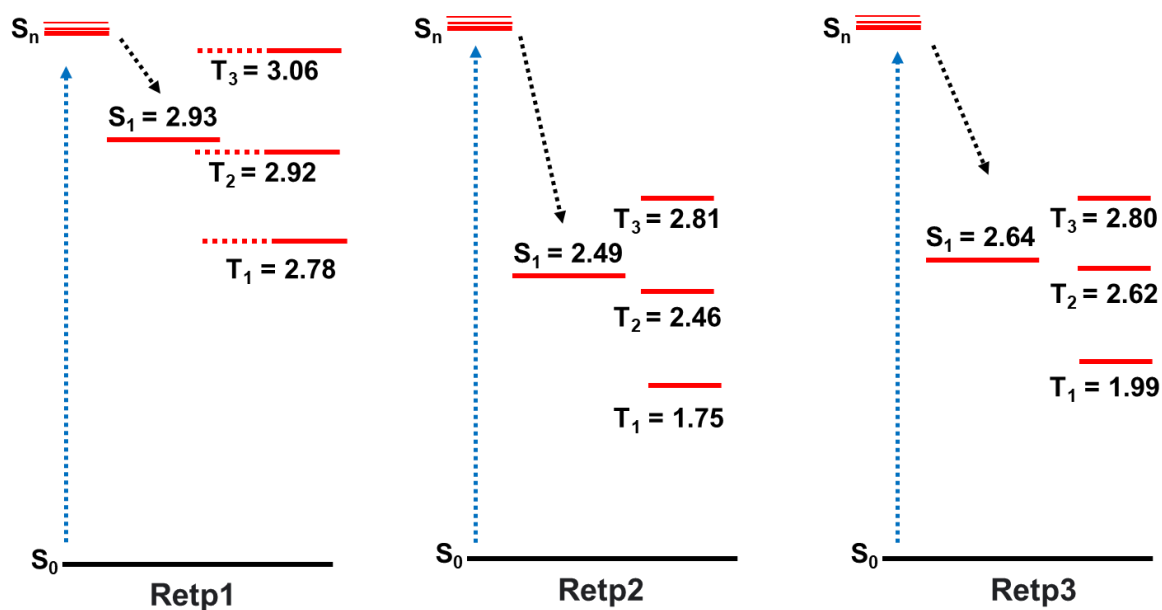


**Figure S21:** Vertical energy levels of the different electronic states of **Retp1-Retp3** obtained from TD-B3LYP/LANL2DZ/6-31g\* in water. All energy values are in eV.

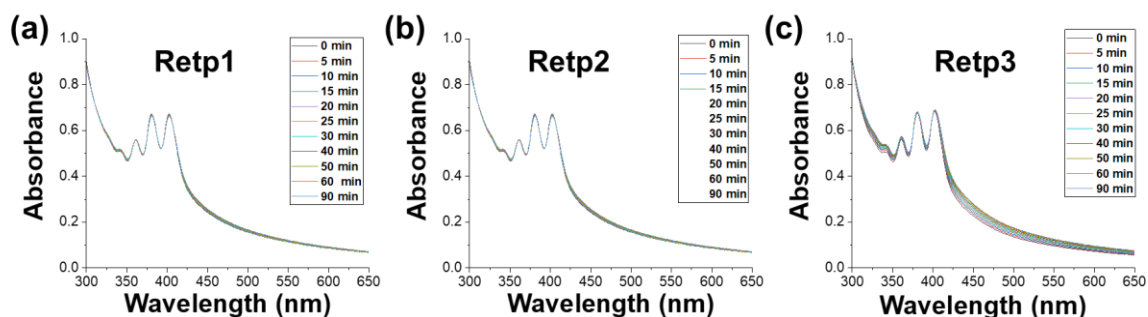


**Figure S22:**  $^1\text{O}_2$  generation by a) **Retp1** (10  $\mu\text{M}$ ) (b) **Retp2** (10  $\mu\text{M}$ ), and **Retp3** (10  $\mu\text{M}$ ) in the dark condition, trapped by DPA,  $^1\text{O}_2$  probe, in DMSO:PBS solution (v/v; 2 : 98).

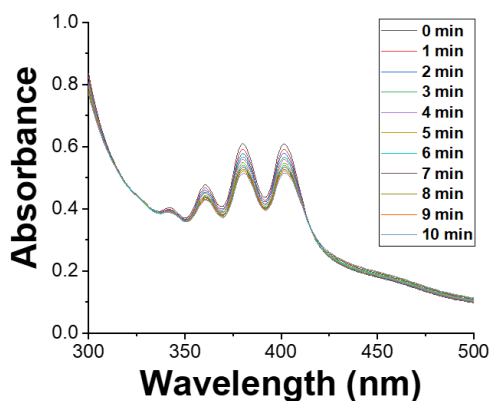


**Figure S23:**  $^1\text{O}_2$  generation by standard  $[\text{Ru}(\text{bpy})_3]\text{Cl}_2$  (10  $\mu\text{M}$ ) under visible light (400-700 nm) exposure, trapped by DPA,  $^1\text{O}_2$  probe, in DMSO:PBS solution (v/v; 2 : 98).

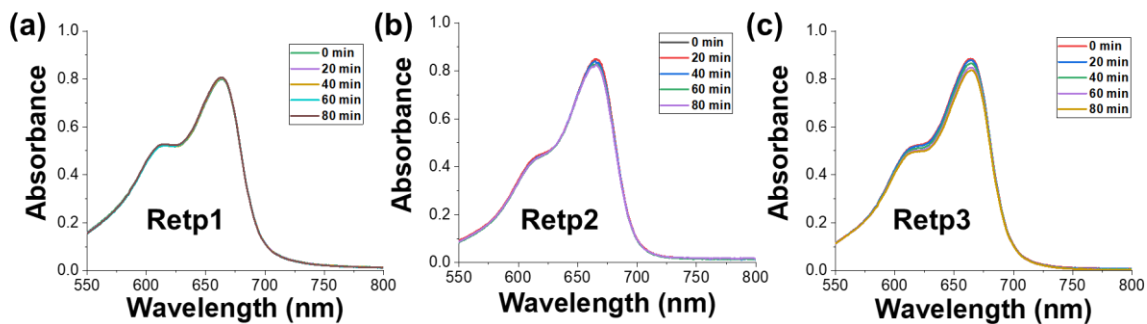


**Figure S24:** OH<sup>•</sup> generation by a) **Retp1** (10 μM) (b) **Retp2** (10 μM), and **Retp3** in the dark condition, trapped by methylene blue (MB), OH<sup>•</sup> probe, in DMSO:PBS solution (v/v; 2 : 98).

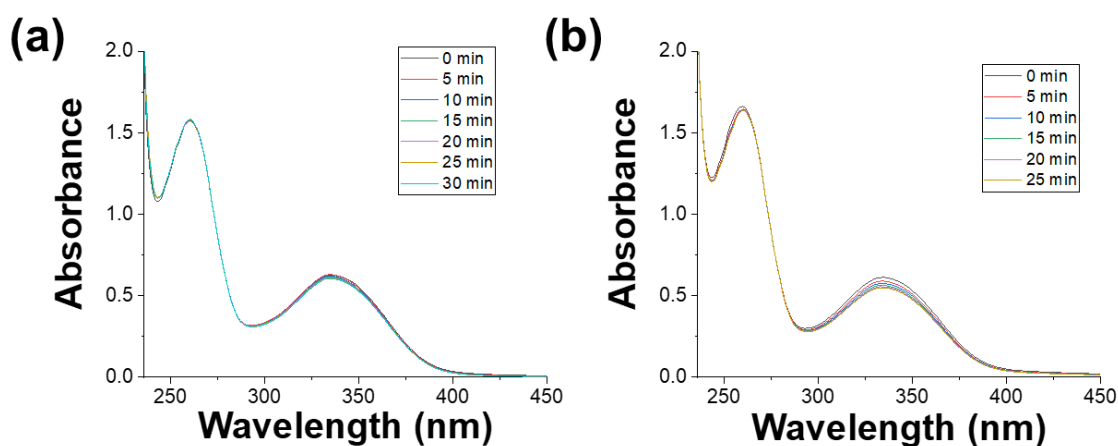


**Figure S25:** Visible light triggered (400-700 nm) NADH (450 μM) oxidation by **Retp1** (15 μM) and **Retp2** (15 μM), recorded in PBS.

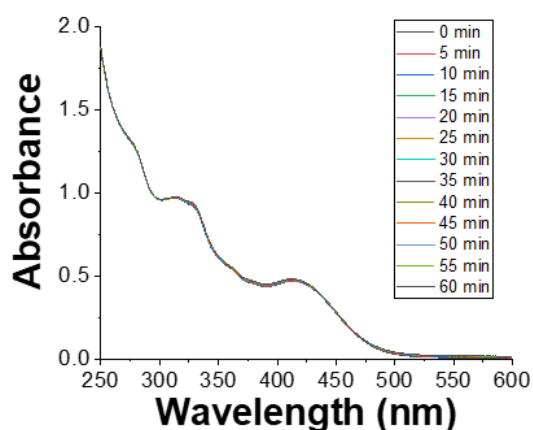


**Figure S26:** Stability plot for **Retp3** under the dark condition.

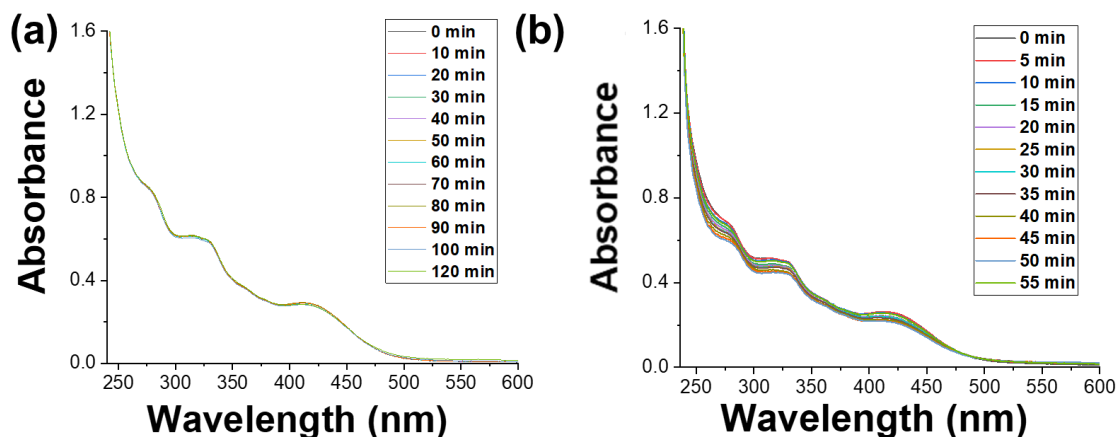


**Figure S27:** Stability plot for **Retp3** under (a) the dark condition and (b) light condition in the presence of 1 mM GSH.

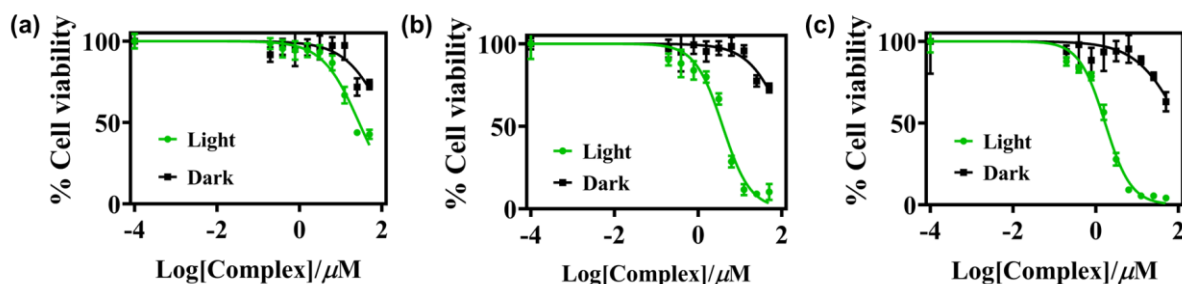


**Figure S28:** Cell viability plots for complexes **Retp1** (a), **Retp2** (b), and **Retp3** (c) in A549 cells after 4 h incubation. One set of cells was exposed to visible light ( $\lambda= 400-700$  nm,  $10$  J  $\text{cm}^{-2}$ ) for 1 h while the other set was kept in the dark. Green and black plots represent light-exposed and dark, respectively.

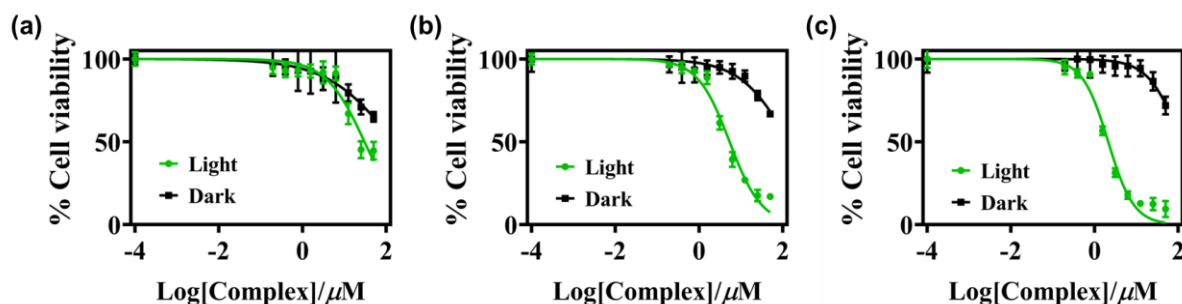


**Figure S29:** Cell viability plots for complexes **Retp1** (a), **Retp2** (b), and **Retp3** (c) in HeLa cells after 4 h incubation. One set of cells was exposed to visible light ( $\lambda= 400-700$  nm,  $10$  J  $\text{cm}^{-2}$ ) for 1 h while the other set was kept in the dark. Green and black plots represent light-exposed and dark, respectively.



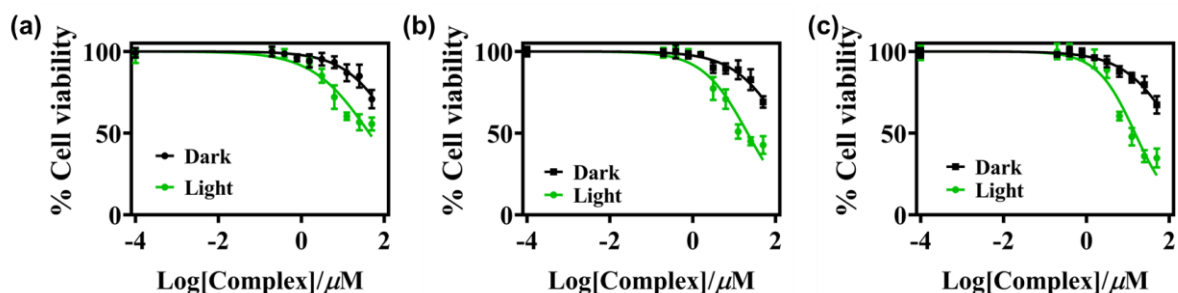


**Figure S30:** Cell viability plots for complexes **Retp1** (a), **Retp2** (b), and **Retp3** (c) in normal human bronchial epithelial BEAS-2B cells after 4 h incubation. One set of cells was exposed to visible light ( $\lambda= 400\text{-}700\text{ nm}$ ,  $10\text{ J cm}^{-2}$ ) for 1 h while the other set was kept in the dark. Green and black plots represent light-exposed and dark, respectively.

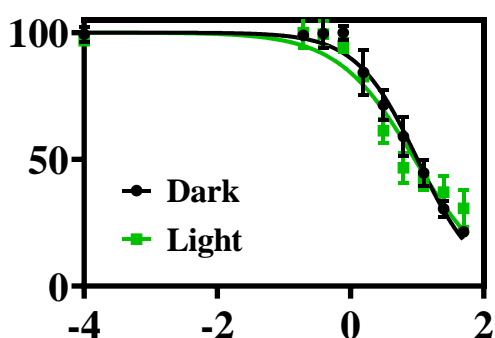


**Figure S31:** Cell viability plots for cisplatin in normal human bronchial epithelial BEAS-2B cells after 4 h incubation. One set of cells was exposed to visible light ( $\lambda= 400\text{-}700\text{ nm}$ ,  $10\text{ J cm}^{-2}$ ) for 1 h while the other set was kept in the dark. Green and black plots represent light-exposed and dark, respectively.

## References

1. J. Wang, and G. S. Hanan, *Synlett*, 2005, **8**, 1251-1254.
2. R. Fernández-Terán, and L. Sévery, *Inorg. Chem.*, 2021, **60**, 1334-1343
3. G. M. Sheldrick, Ver. 2.05, University of Göttingen, Göttingen, Germany, **2002**.
4. G. M. Sheldrick, *Acta Cryst.*, 2015, **71**, 3-8.
5. O. V. Dolomanov, L. J. Bourhis, R. J. Gildea, J. A. K. Howard, and H. Puschmann, *J. Appl. Cryst.*, 2009, **42**, 339-341.
6. G. M. Sheldrick, *Acta Cryst.*, 2008, **64**, 112-122.
7. L. J. Farrugia, *J. Appl. Crystallogr.*, 1997, **30**, 565.
8. C. F. Macrae, I. Sovago, S. J. Cottrell, P. T. A. Galek, P. McCabe, E. Pidcock, M. Platings, G. P. Shields, J. S. Stevens, M. Towler, and P. A. Wood, *J. Appl. Cryst.*, 2020, **53**, 226-235.
9. S. P. Westrip, *J. Appl. Cryst.*, 2010, **43**, 920-925.
10. M. J. Frisch, G. W. Trucks, H. B. Schlegel, G. E. Scuseria, J. R. Cheeseman, G. Scalmani, S. V. Barone, G. A. Petersson, H. Nakatsuji, X. Li, M. Caricato, A. V. Marenich, J. Bloino, B. G. Janesko, R. Gomperts, B. Mennucci, H. P. Hratchian, J. V. Ortiz, A. F. Izmaylov, J. L. Sonnenberg, D. Williams-Young, F. Ding, F. Lipparini, F. Egidi, J. Goings, B. Peng, A. Petrone, T. Henderson, D. Ranasinghe, V. G. Zakrzewski, J. Gao, N. Rega, G. Zheng, W. Liang, M. Hada, M. Ehara, K. Toyota, R. Fukuda, J.

Hasegawa, M. Ishida, T. Nakajima, Y. Honda, O. Kitao, H. Nakai, T. Vreven, K. Throssell, J. A. Montgomery Jr., J. E. Peralta, F. Ogliaro, M. J. Bearpark, J. J. Heyd, E. N. Brothers, K. N. Kudin, V. N. Staroverov, T. A. Keith, R. Kobayashi, J. Normand, K. Raghavachari, A. P. Rendell, J. C. Burant, S. S. Iyengar, J. Tomasi, M. Cossi, J. M. Millam, M. Klene, C. Adamo, R. Cammi, J. W. Ochterski, R. L. Martin, K. Morokuma, O. Farkas, J. B. Foresman, and D. J. Fox, Gaussian 16 Rev. A.03, Wallingford, CT, **2016**.